



Microwave dielectrics: solid solution, ordering and microwave dielectric properties of $(1-x)\text{Ba}(\text{Mg}_{1/3}\text{Nb}_{2/3})\text{O}_3-x\text{Ba}(\text{Mg}_{1/8}\text{Nb}_{3/4})\text{O}_3$ ceramics

YOGITA BISHT¹, RICHA TOMAR¹, PULLANCHIYODAN ABHILASH²,
DEEPA RAJENDRAN LEKSHMI² and M THIRUMAL^{1,*}

¹Department of Chemistry, University of Delhi, Delhi 110007, India

²Materials Science and Technology Division, National Institute for Interdisciplinary Science and Technology (NIIST-CSIR), Industrial Estate, Trivandrum 695019, India

*Author for correspondence (thirumalm@hotmail.com)

MS received 12 March 2016; accepted 25 January 2017; published online 5 September 2017

Abstract. The effect of $\text{Ba}(\text{Mg}_{1/8}\text{Nb}_{3/4})\text{O}_3$ phase on structure and dielectric properties of $\text{Ba}(\text{Mg}_{1/3}\text{Nb}_{2/3})\text{O}_3$ was studied by synthesizing $(1-x)\text{Ba}(\text{Mg}_{1/3}\text{Nb}_{2/3})\text{O}_3-x\text{Ba}(\text{Mg}_{1/8}\text{Nb}_{3/4})\text{O}_3$ ($x = 0, 0.005, 0.01$ and 0.02) ceramics. Superlattice reflections due to 1:2 ordering appear as low as 1000°C . $\text{Ba}(\text{Mg}_{1/3}\text{Nb}_{2/3})\text{O}_3$ forms solid solution with $\text{Ba}(\text{Mg}_{1/8}\text{Nb}_{3/4})\text{O}_3$ for all 'x' values studied until 1350°C . Ordering was confirmed by powder X-ray diffraction pattern, Raman study and HRTEM. Ceramic pucks can be sintered to density $>92\%$ of theoretical density. Temperature and frequency-stable dielectric constant and nearly zero dielectric loss ($\tan \delta$) were observed at low frequencies (20 MHz). The sintered samples exhibit dielectric constant (ϵ_r) between 30 and 32, high quality factor between 37000 and 74000 GHz and temperature coefficient of resonant frequency (τ_f) between 21 and 24 ppm $^\circ\text{C}^{-1}$.

Keywords. Resonators; complex perovskites; X-ray diffraction; dielectric properties; high Q .

1. Introduction

$\text{Ba}(\text{B}'_{1/3}\text{B}''_{2/3})\text{O}_3$ ($\text{B}' = \text{Zn, Mg, Ni, Co}$ and $\text{B}'' = \text{Ta, Nb}$)-based perovskite oxides are used in microwave dielectrics, which have application in wireless communications. Their high permittivity (ϵ_r), high quality factor (Q.f.) and near-zero temperature coefficient of resonant frequency (τ_f) make them excellent candidates for filters and resonators at base station. Here, Ta^{5+} and Nb^{5+} are used as transition metal ions with low-lying d^0 orbital mix with the orbital of ligands and create multiple coordination with oxygen [1]. This improves polarizability of these elements and they also provide opportunities of compositional tuning by the substitutional flexibility of B-site cations. Normally, among all the known $\text{Ba}(\text{B}'_{1/3}\text{B}''_{2/3})\text{O}_3$ ($\text{B}' = \text{Zn, Mg, Ni, Co}$ and $\text{B}'' = \text{Ta, Nb}$) perovskites, tantalates show much better Q.f. as compared with niobates. However, Ta^{5+} is comparatively expensive; hence, to reduce the cost of dielectric resonators and to understand the chemistry, niobates are explored as the logical substitute for tantalates. $\text{Ba}(\text{Mg}_{1/3}\text{Nb}_{2/3})\text{O}_3$ (BMN) is one such ceramic that draws attention due to its good dielectric properties $\epsilon_r = 32$, $Q = 5600$ (10.5 GHz) and $\tau_f = 33$ ppm $^\circ\text{C}^{-1}$ [2]. The $\text{A}(\text{B}_{1/3}\text{B}'_{2/3})\text{O}_3$ -type ceramics have been reported to have three kinds of ordered structures depending upon the arrangement of B-site

cations:

- (i) disordered cubic structure with space group $\text{Pm}\bar{3}\text{m}$ (O_h^1), lattice parameter $a \sim 4 \text{ \AA}$;
- (ii) 1:1 ordered cubic structure with space group $\text{Fm}\bar{3}\text{m}$ (O_h^5); here, the unit cell lattice parameter is twice that of the disordered cubic structure, i.e., $a \sim 8 \text{ \AA}$;
- (iii) 1:2 ordered hexagonal structure with space group $\text{P}\bar{3}\text{m}1$ (D_3^3d), lattice parameters $a \sim 5.7 \text{ \AA}$ and $c \sim 7 \text{ \AA}$.

Among these, 1:2 ordered hexagonal structure is desirable as it is reported to have better Q.f. as compared with others. This kind of 1:2 ordering was first reported by Galasso and Pyle [3] in $\text{Ba}(\text{Sr}_{1/3}\text{Ta}_{2/3})\text{O}_3$. They described its structure as a repetition of three close-packed BaO_3 layers with Sr^{2+} and Ta^{5+} in an ordered arrangement with a $\{\text{Sr}^{2+}.. \text{Ta}^{5+}.. \text{Ta}^{5+}\}$ repeated sequence in octahedral hole. This kind of 1:2 ordering of B-site cations expands the original perovskite unit cell along $\langle 111 \rangle$ direction and contracts it along the direction normal to $\langle 111 \rangle$, which produces superstructure reflections and deviation of c/a ratio from $\sqrt{3}/2$ (1.2247), the ideal value for hexagonal structure.

It is not easy to observe superlattice reflections related to 1:2 ordering in Nb system as the scattering power of Nb is lower than that of Ta due to lower atomic number of Nb^{5+} than that of Ta^{5+} [4,5]. Galasso and Pyle [6]

reported 1:2 ordered structure for BMN with lattice parameter $a = 5.77 \text{ \AA}$ and $c = 7.08 \text{ \AA}$ for samples sintered at 1400°C . For the BMN system, 1:2 ordering normally starts around 1400°C and completely ordered structure can be obtained at higher temperatures; beyond this the structure disorders. High-temperature treatment also results into secondary phases that deteriorate dielectric properties. Kolodiaznyy *et al* [7] reported ordering for BMN ceramics at 1620°C , along with $\text{Ba}_3\text{Nb}_5\text{O}_{15}$ secondary phase. Janaswamy *et al* [8] did not get completely ordered BMN. At 1300°C , they reported completely disordered cubic structure for BMN; however, in a temperature range between 1400 and 1600°C , they observed a mixture of disordered cubic and ordered trigonal structure. Vittayakorn and Roongtao [9] also confirm the onset of 1:2 ordering in BMN at 1400°C . Jae-Gwan Park Kim *et al* [10] studied the effect of sintering temperature and duration on structure and dielectric properties of BMN; they sintered BMN at three different conditions: 1350°C for 4 h, 1500°C for 4 h and 1350°C for 40 h; they reported that although overall 1:2 ordering was maintained in all the ceramics, the ceramics sintered at higher temperature or for longer duration showed local disordering.

There are several reports about substitutions in BMN to improve the ordering, sintering and dielectric properties [11–20]. Here we report the synthesis of $(1-x)\text{Ba}(\text{Mg}_{1/3}\text{Nb}_{2/3})\text{O}_3-x\text{Ba}(\text{Mg}_{1/8}\text{Nb}_{3/4})\text{O}_3$ to explore the influence of $\text{Ba}(\text{Mg}_{1/8}\text{Nb}_{3/4})\text{O}_3$ on $\text{Ba}(\text{Mg}_{1/3}\text{Nb}_{2/3})\text{O}_3$ in forming the solid solution, 1:2 ordering, sintering and its effect on dielectric properties.

2. Experimental

Oxides of $(1-x)\text{Ba}(\text{Mg}_{1/3}\text{Nb}_{2/3})\text{O}_3-x\text{Ba}(\text{Mg}_{1/8}\text{Nb}_{3/4})\text{O}_3$ ($x = 0, 0.005, 0.01$ and 0.02) were prepared by solid-state method. BaCO_3 (99+%, Sigma-Aldrich), MgO (>99+%, Sigma-Aldrich) and Nb_2O_5 (99%, Alfa Aesar) were used as starting materials. These starting materials were dried, weighed according to the stoichiometry and mixed using an agate mortar and a pestle with acetone as a solvent. The powders were calcined at 1000°C for about 72 h in an alumina crucible with intermittent grindings. The powders were compacted into pellets using an uniaxial press and heat treated further at 1200°C for 24 h, with intermittent grinding and compacting after confirming the phase. The final powders were compacted and sintered at 1350°C for 12 h.

The powder X-ray diffraction (XRD) patterns were collected on a Bruker D8 Discover X-ray diffractometer using $\text{Cu-K}\alpha$ radiation generated at 40 kV and 40 mA. The data were collected in the 2θ range of 10 – 60° with step scanning mode of 0.02° per step at 1° min^{-1} . The Raman spectra of the samples were recorded at room temperature using a Renishaw Invia Raman Spectrometric Analyser. The excitation source was the 2.5 mW output of the 514.5 nm line of an Ar^+ ion laser. The obtained Raman spectra exhibited resolution of $\sim 0.5 \text{ cm}^{-1}$. Transmission electron microscopy

(TEM) (model TECNAI G²T30 operating at 50–300 kV) was used for imaging. A scanning electron microscope (SEM) (Model 6610LV, JEOL, Tokyo, Japan) was used for microstructure analysis; the pellets were thermally etched and coated with Au–Pd coating using a JEOL, JEC—3000 FC Auto fine coater before SEM measurement to make the surface conducting. Low-frequency dielectric properties were measured using a C50 Alpha-A high performance frequency analyser (Novocontrol Broadband, Novocontrol Technologies) over frequency ranges of 500 kHz, 1 MHz, 10 MHz, 15 MHz and 20 MHz, and temperature range of -20 to 100°C with intervals of 30°C . A Vector Network Analyser (Model No. E5071C ENA series; Agilent Technologies, Santa Clara, CA) was used to measure dielectric properties in the frequency range of 6–12 GHz. The Hakki–Coleman method was used to measure relative permittivity (ϵ_r) and temperature coefficient of resonant frequency (τ_f) in the temperature range of 25 – 70°C . The unloaded Q.f. was measured by the resonant cavity method [21].

3. Results and discussion

The powder X-ray diffraction patterns (PXRD) of $(1-x)\text{Ba}(\text{Mg}_{1/3}\text{Nb}_{2/3})\text{O}_3-x\text{Ba}(\text{Mg}_{1/8}\text{Nb}_{3/4})\text{O}_3$ samples ($x = 0, 0.005, 0.01$ and 0.02) calcined at 1000°C for 72 h are shown in figure 1. The powder XRD patterns show superlattice reflections corresponding to (100) of P-3m1 at 1000°C . The 1:2 ordering at this low temperature by solid-state method was not reported earlier. However, for $x = 0.02$, the PXRD pattern shows the presence of $\text{Ba}_5\text{Nb}_4\text{O}_{15}$ at 1000°C , suggesting that a biphasic region exists as the ‘ x ’ increases. To check the phase compatibility with ‘ x ’ the temperature was further increased to 1200°C . The increase in temperature, apart from improving the intensity of 1:2 superstructure reflections, also leads into a different biphasic region, corresponding

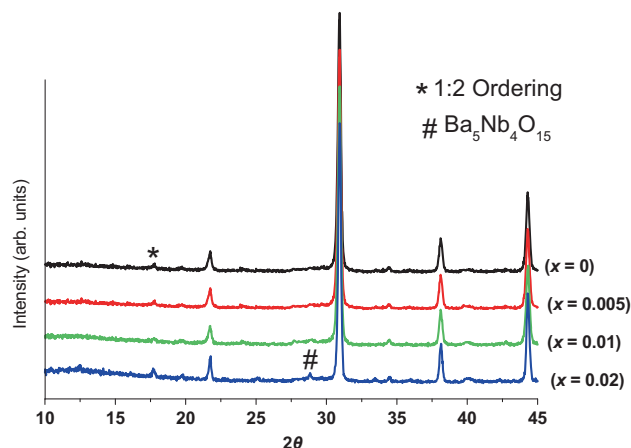


Figure 1. Powder X-ray diffraction patterns of $(1-x)\text{Ba}(\text{Mg}_{1/3}\text{Nb}_{2/3})\text{O}_3-x\text{Ba}(\text{Mg}_{1/8}\text{Nb}_{3/4})\text{O}_3$ powder calcined at 1000°C for 72 h.

to Ba(Mg_{1/3}Nb_{2/3})O₃ and Ba(Mg_{1/8}Nb_{3/4})O₃ at 29.5° 2θ as shown in figure 2. The Ba(Mg_{1/8}Nb_{3/4})O₃ phase lies on the tie line between Ba(Mg_{1/3}Nb_{2/3})O₃ and Ba₅Nb₄O₁₅ in the BaO–MgO–Nb₂O₅ ternary phase diagram.

The powders were compacted and sintered at 1350°C for 12 h. The density of all the pellets was >92% of the theoretical density. The PXRD pattern taken on the surface of the sintered pellet is shown in figure 3. Here the intensity of superlattice reflections further improved and all the sintered pellets and the powder pattern also show the presence of (001) reflections and enhancement of 1:2 ordering. The appearance of a peak at

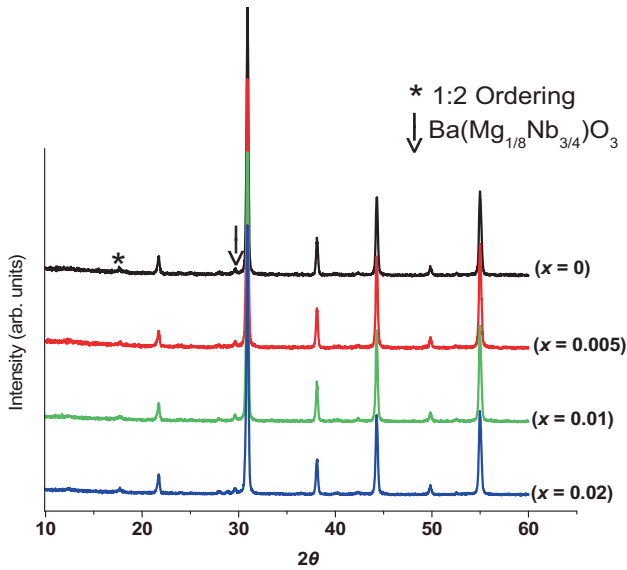


Figure 2. Powder X-ray diffraction patterns of (1-x)Ba(Mg_{1/3}Nb_{2/3})O₃-xBa(Mg_{1/8}Nb_{3/4})O₃ at 1200°C.

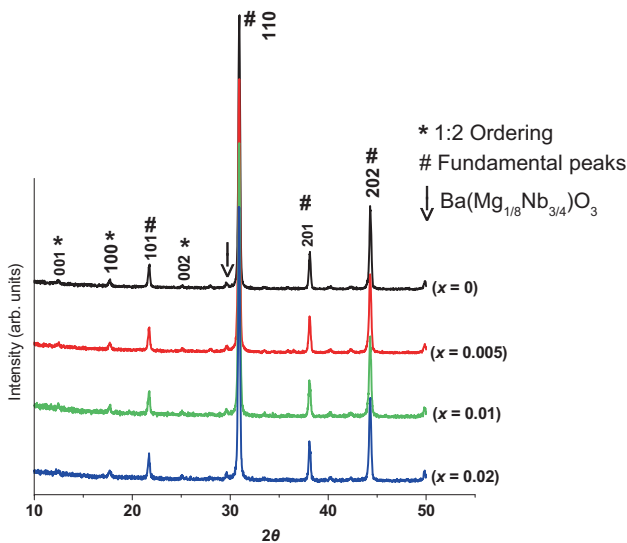


Figure 3. Powder X-ray diffraction patterns of (1-x)Ba(Mg_{1/3}Nb_{2/3})O₃-xBa(Mg_{1/8}Nb_{3/4})O₃ on pellet surface at 1350°C.

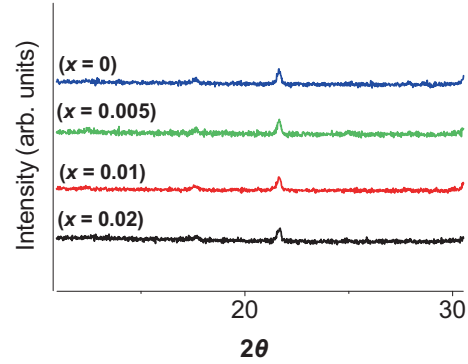


Figure 4. Powder X-ray diffraction patterns of (1-x)Ba(Mg_{1/3}Nb_{2/3})O₃-xBa(Mg_{1/8}Nb_{3/4})O₃ at low angle on the pellet sintered at 1350°C, showing ordering and solid solution.

~29.5° 2θ is similar to that of Ba(Zn_{1/3}Ta_{2/3})O₃ at the surface of the sintered pellets [22,23].

The PXRD pattern on the crushed pellets was obtained to explore the influence of Ba(Mg_{1/8}Nb_{3/4})O₃ on Ba(Mg_{1/3}Nb_{2/3})O₃ and to study the extent of solid solution. Figure 4 clearly shows the presence of 1:2 ordering and absence of reflection at ~29.5° 2θ, implying that Ba(Mg_{1/8}Nb_{3/4})O₃ influences the solid solution formation for this system till x = 0.02.

The 1:2 ordering was quantified using the ordering parameter *S*. This ordering parameter is expressed in terms of relative intensity of highest intensity superlattice reflection against highest intensity fundamental reflection.

$$S = \left(\frac{(I_{100}/I_{110,012})_{\text{obs}}}{(I_{100}/I_{110,012})_{\text{ordered}}} \right)^{1/2},$$

where $(I_{100}/I_{110,012})_{\text{obs}}$ is the ratio of the observed intensity of (100) superstructure reflection to that of (110) and (012) subcell reflection peaks. The values of the observed intensities I_{100} and $I_{110,012}$ can be calculated from the area of the corresponding XRD peaks [24]. The value of $(I_{100}/I_{110,012})_{\text{ordered}}$ for fully ordered BMN was earlier reported as 0.0316 [25] and 0.0304 [7]. Lattice distortion can be quantified by the ratio of lattice parameters, i.e., c/a . Higher the deviation of c/a from $(3/2)^{1/2}$, higher the lattice distortion. Therefore c/a ratio should be higher than 1.2247 for a well-ordered structure. Figure 5 shows the variation of $(I_{100}/I_{110,012})_{\text{obs}}$ and c/a with 'x'.

Here, both ordering parameter and c/a ratio increase till $x=0.01$ and then decrease for $x=0.02$. The 1:2 ordering was further confirmed by Raman study. The Raman spectra of A(B_{1/3}B'_{2/3})O₃-type ceramics were reported earlier by Siny *et al* [26]. For 1:2 ordered structure with space group P-3m1, three weak lines should be present in the 150–300 cm⁻¹ interval of Raman spectra. Figure 6 shows the Raman spectra of the crushed powders for all the 'x' values after sintering.

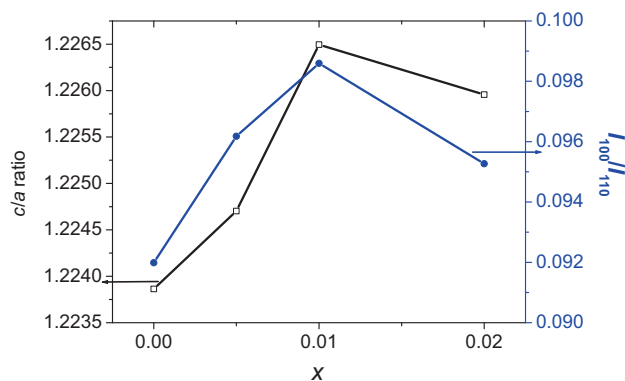


Figure 5. Variation of c/a ratio and integrated intensity ratio of (I_{100}/I_{110}) with x .

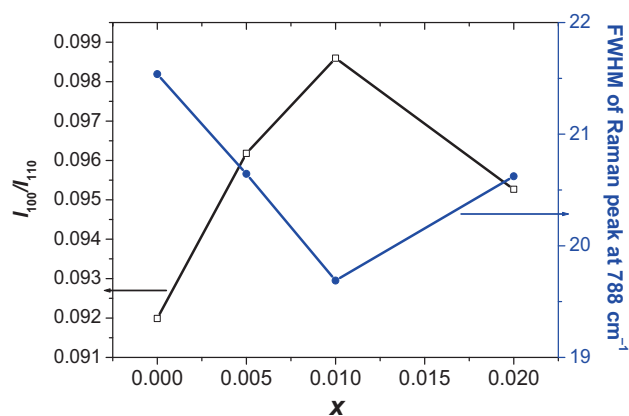


Figure 7. Comparison of FWHM of Raman peak at 788 cm^{-1} ($A_{1g}(O)$ mode) and integrated intensity ratio (I_{100}/I_{110}) with x .

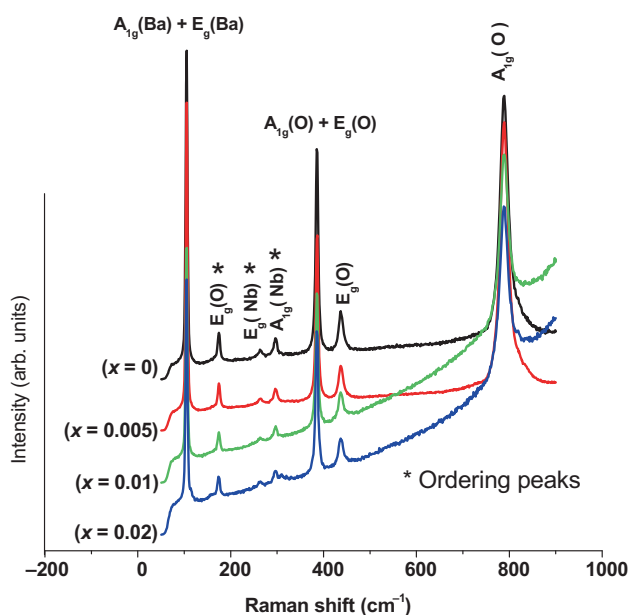


Figure 6. Raman spectra of $(1-x)\text{Ba}(\text{Mg}_{1/3}\text{Nb}_{2/3})\text{O}_3-x\text{Ba}(\text{Mg}_{1/8}\text{Nb}_{3/4})\text{O}_3$ after sintering at 1350°C .

Here, three weak peaks between 150 and 300 cm^{-1} were present, indicating the presence of 1:2 ordering for all the 'x' values under study.

In the Raman spectra, the FWHM (full-width at half maximum) of the peak at 788 cm^{-1} follows exactly reverse trend as that of integrated intensity ratio. Figure 7 shows that the FWHM decreases till $x = 0.01$ and then increases for $x = 0.02$. Both FWHM of Raman peak at 788 cm^{-1} ($A_{1g}(O)$ mode) and integrated intensity ratio are indicative of dielectric loss and Q.f. of $A(B'_{1/3}B''_{2/3})\text{O}_3$ -type ceramic. In the Raman spectroscopy, FWHM is related to phonon lifetime. Smaller the FWHM, narrower the peak, which results in longer phonon life and lesser phonon interaction. Raman-active samples with poor ordering show broad peak and large phonon interaction.

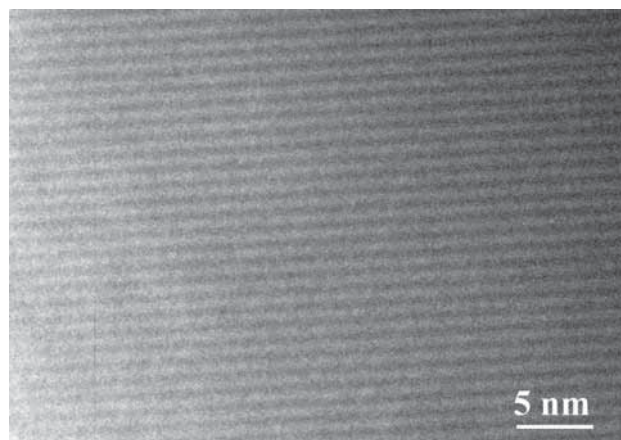


Figure 8. HRTEM lattice fringes of $x = 0.005$ sample.

Better interaction results in large energy consumption and poor Q.f. [27].

The HRTEM images at all compositions studied show 1:2 ordering. Figure 8 shows the HRTEM image for $x = 0.005$, of the crushed pellet exhibiting lattice fringes with interplanar distance (d -spacing) indicative of 1:2 ordered structure; similar patterns were observed for all the x values. Figure 9 shows the SEM image of thermally etched pellet of $x = 0.005$ composition; all the samples show similar type of grains. The particles are similar to that of cubic perovskites and highly compact; there was no evidence for the presence of grains representing hexagonal perovskites. The density of the pellets was $>92\%$ theoretical.

The dielectric constant and the dielectric loss ($\tan \delta$) of all the compositions in this study were measured over the frequency range 500 kHz – 20 MHz and temperature range 70 to -20°C . The dielectric constant for all compositions was found to be stable with respect to temperature and frequency. The dielectric loss for all the compositions was nearly zero at all frequencies and in all temperature regions studied.

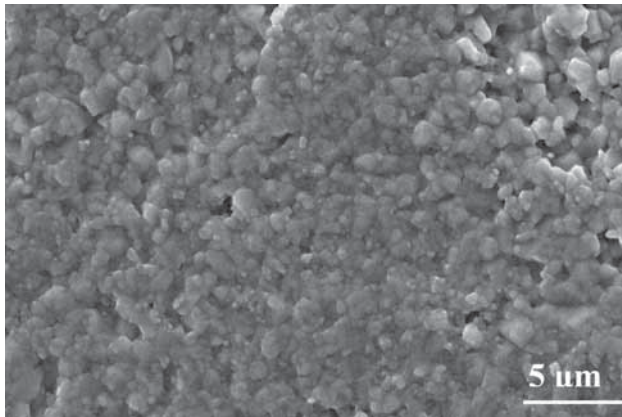


Figure 9. SEM image of $x = 0.005$ sample.

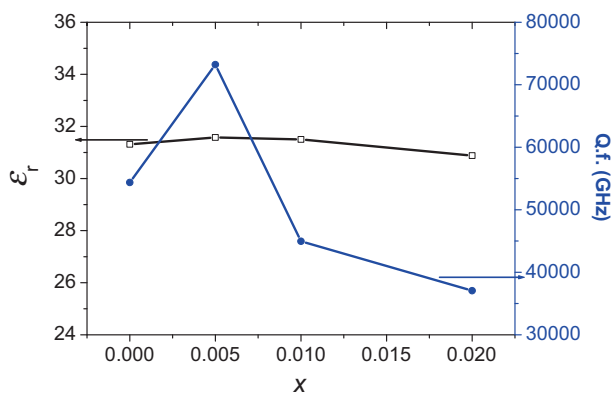


Figure 10. Variation of Q.f. and ϵ_r with x .

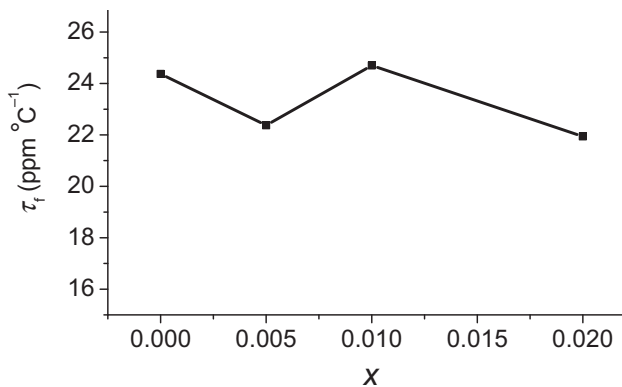


Figure 11. Variation of τ_f with x .

The dielectric properties at GHz frequencies are shown in figure 10; the dielectric constant remains almost constant for the entire composition studied.

Figure 10 also shows the variation of Q.f. with ' x '. High Q.f. values are observed for all the compositions. It is interesting to note that despite higher 1:2 ordering parameter and c/a value for $x = 0.01$ as compared with $x = 0.005$, Q.f. is higher for $x = 0.005$. This shows that Q.f. depends not only

on 1:2 ordering but also on other factors like microcracks and processing; other defects may also play a vital role in Q.f. [28]. Figure 11 shows the variation of τ_f with ' x '; τ_f varies between 21 and 24 ppm °C⁻¹.

4. Conclusion

$(1-x)\text{Ba}(\text{Mg}_{1/3}\text{Nb}_{2/3})\text{O}_3-x\text{Ba}(\text{Mg}_{1/8}\text{Nb}_{3/4})\text{O}_3$ ($0 \leq x \leq 0.02$) was synthesized by solid-state method to explore the influence of $\text{Ba}(\text{Mg}_{1/8}\text{Nb}_{3/4})\text{O}_3$ in forming the solid solution and 1:2 ordering, and also sintering and its effect on dielectric properties of $\text{Ba}(\text{Mg}_{1/3}\text{Nb}_{2/3})\text{O}_3$. The pure phase of $\text{Ba}(\text{Mg}_{1/8}\text{Nb}_{3/4})\text{O}_3$ itself is not known in the literature. Superlattice reflections due to 1:2 ordering appear at as low as 1000°C. $\text{Ba}(\text{Mg}_{1/3}\text{Nb}_{2/3})\text{O}_3$ forms solid solution with $\text{Ba}(\text{Mg}_{1/8}\text{Nb}_{3/4})\text{O}_3$ for all ' x ' values studied until 1350°C. Ordering was confirmed by powder XRD, Raman study and HRTEM. Quantification of 1:2 ordering in the form of ratio of integrated intensity and lattice distortion (c/a) shows increase in ordering till $x = 0.01$. Nearly zero dielectric loss ($\tan \delta$) was observed at low frequency up to 20 MHz. The microwave dielectric properties of sintered samples show dielectric constant (ϵ_r) around 31 for all the ' x ' values and high Q.f. between 37000 and 74000 GHz with the maximum Q.f. at $x = 0.005$. The temperature coefficient of resonant frequency (τ_f) varies between 21 and 24 ppm °C⁻¹.

Acknowledgements

This work was supported by DST through SR/S1/PC-09/2010 and University of Delhi. Yogita Bisht acknowledges UGC.

References

- [1] Grebennikov D and Mascher P 2011 *J. Mater. Res.* **26** 1116
- [2] Nomura S 1983 *Ferroelectrics* **49** 61
- [3] Galasso F and Pyle J 1963 *J. Phys. Chem.* **67** 533
- [4] Cullity B D and Stock S R 2001 *Elements of X-ray diffraction*, 3rd edn (Upper Saddle River, NJ: Prentice-Hall)
- [5] Hughes H, Iddles D M and Reaney I M 2001 *Appl. Phys. Lett.* **79** 2952
- [6] Galasso F and Pyle J 1963 *J. Phys. Chem.* **67** 1561
- [7] Kolodiaznyh K, Petric A, Belous A, V'yunov O and Yanchevskij O 2002 *J. Mater. Res.* **17** 3182
- [8] Janaswamy S, Murthy G S, Dias E D and Murthy V R K 2002 *Mater. Lett.* **55** 414
- [9] Vittayakorn W and Roongtao R 2011 In C Sikalidis (Ed) *Advances in ceramics: synthesis and characterization, processing and specific applications* ISBN 978-953-307-505-1
- [10] Kim Y W, Park J H and Park J G 2004 *J. Eur. Ceram. Soc.* **24** 1775
- [11] Yoon K H, Jung B J and Kim E S 1989 *J. Mater. Sci. Lett.* **8** 819
- [12] Thirumal M and Ganguli A K 2000 *Bull. Mater. Sci.* **23** 495

- [13] Akbas M A and Davies P K 1998 *J. Am. Ceram. Soc.* **81** 2205
- [14] Park H M, Lee H J, Cho Y K and Nahm S 2003 *J. Mater. Res.* **18** 1003
- [15] Liu H X, Tian Z Q, Wang H, Yu H T and Ouyang S X 2004 *J. Mater. Sci.* **39** 4319
- [16] Tian Z Q, Liu H X, Yu H T and Ouyang S X 2004 *Mater. Chem. Phys.* **86** 228
- [17] Akbas M A and Davies P K 1998 *J. Am. Ceram. Soc.* **81** 670
- [18] Veres A, Marinel S and Roulland F 2005 *J. Eur. Ceram. Soc.* **25** 2759
- [19] Lim J B, Son J O, Nahm S, Lee W S, Yoo M J, Gang N G *et al* 2004 *Jpn. J. Appl. Phys.* **43** 5388
- [20] Dias A, Matinaga F M and Moreira R L 2007 *Chem. Mater.* **19** 2335
- [21] Sebastian M T 2008 *Dielectric materials for wireless communication* (Oxford, U.K.: Elsevier)
- [22] Thirumal M and Davies P K 2005 *J. Am. Ceram. Soc.* **88** 2126
- [23] Davies P K, Borisevich A and Thirumal M 2003 *J. Eur. Ceram. Soc.* **23** 2461
- [24] Matsumoto K, Hiuga T, Takada K and Ichimura H 1986 *Proceedings of the 6th IEEE international symposium on applications of ferroelectrics* 118
- [25] Dias A, Ciminelli V S T, Matinaga F M and Moreira R L 2001 *J. Eur. Ceram. Soc.* **21** 2739
- [26] Siny I G, Tao R, Katiyar R S, Guo R and Bhalla A S 1998 *J. Phys. Chem. Solids* **59** 181
- [27] Wang C H and Jing X P 2009 *J. Am. Ceram. Soc.* **92** 1547
- [28] Ra S H and Phulé P P 1999 *J. Mater. Res.* **14** 4259